

Hi Sebastian,

Responses below.

1) Could you make a figure like Fig. 2 in your response, but with the angle θ_{nq} (Lab) on the vertical axis? In other words, plot the distribution of events in both angle (relative to q) and magnitude of the missing momentum in the lab frame, after all your cuts (the ones you propose to use, which I assume does NOT include the W cut anymore, just on W_n). I just have a very hard time relating the mix of lab and cm variables you plotted to something my brain can grasp. Ideally I'd like to see 2 versions of the plots - with and without the cut on $p(e')$. It might be helpful (but not necessary) if you could also produce the plots showing lines of constant x_{Bj} on the same 2-D space (p_{miss} vs. θ_{nq}) that you described to me in words.

The first two plots below shows the effect of the $\Delta p_e < 0.015$ GeV/c cut on the θ_{pq} versus p_m distribution (where θ_{pq} is in the lab) for the reversed torus polarity data. The Δp_e

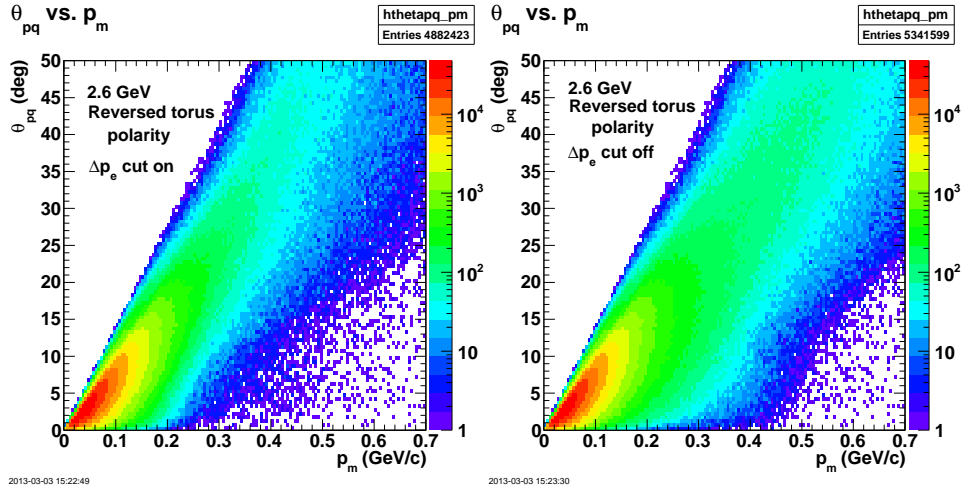


Figure 1: Comparison of θ_{pq} versus p_m distribution with (left-hand panel) and without (right-hand panel) the Δp_e cut for the reversed torus polarity data.

cut removes electrons with momenta below the value expected with no radiative effects so the measured momentum transfer $\vec{q} = \vec{p}_{beam} - \vec{p}_e$ is greater than expected with no radiation. The missing momentum is $\vec{p}_m = \vec{q} - \vec{p}_p$ where \vec{p}_p is the proton 3-momentum and p_m tends to have a greater magnitude than expected with no radiation. In the left-hand panel of Fig 1, the high- p_m side of the distribution for a particular value of θ_{pq} is reduced when the Δp_e cut is used. Fig. 2 shows the same attributes for the normal torus polarity data.

To demonstrate the kinematic range of our data we plotted lines of constant x_{Bj} on the 2-dimensional, θ_{pq} - p_m distributions with the full set of cuts (Figs 3-4). The curves in the left-hand panel of Fig. 3, for example, mark the low- p_m side of the main 'ridge' in the θ_{pq} - p_m distribution. The $x_{Bj} = 1$ curve (solid) starts at $\theta_{pq} = 0^\circ$, follows the low- p_m limit of the measured distribution up to $\theta_{pq} \approx 50^\circ$ and then the cross section for these kinematics

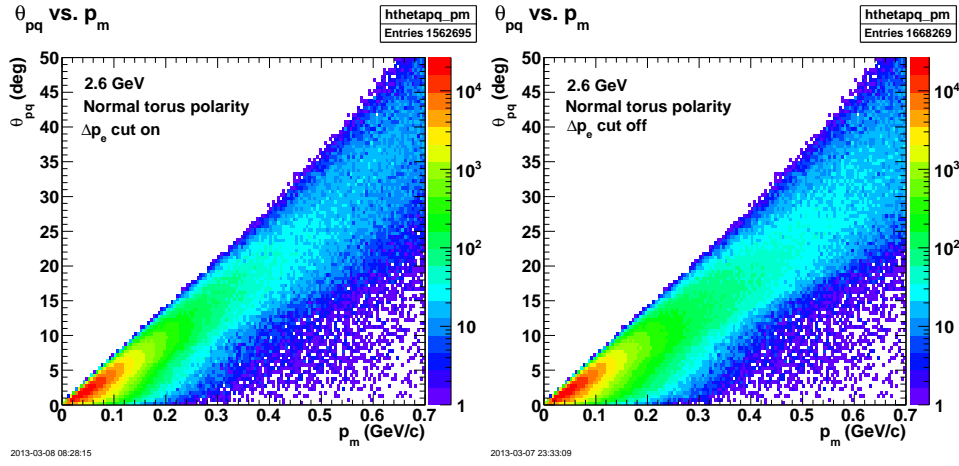


Figure 2: Same as previous plot except for the normal torus polarity data.

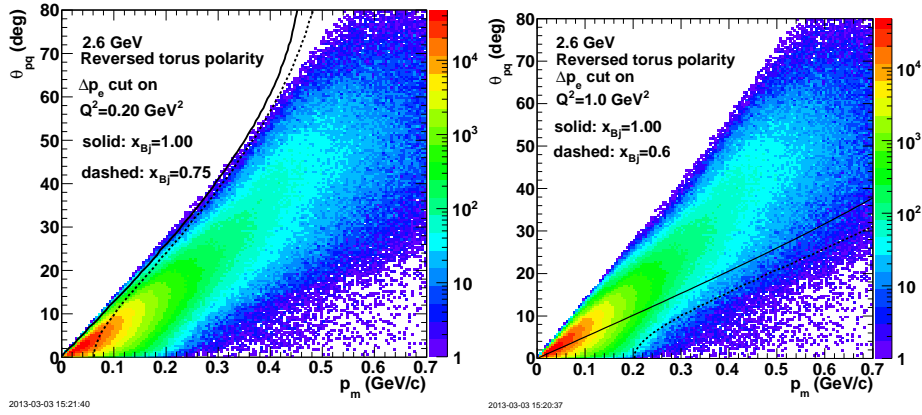


Figure 3: Distribution of θ_{pq} versus p_m showing kinematic relationship at the Q^2 and x_{Bj} limits of the 2.6-GeV, reversed torus polarity data

goes away. The $x_{Bj} = 0.75$ curve (dashed) marks the high- p_m limit for this value of Q^2 . Kinematics with $x_{Bj} > 1.0$ lie in between the the solid and dashed curves in each panel. The high- Q^2 behavior of the kinematics is shown in the right-hand panel. The $x_{Bj} = 1$ curve (solid) starts at $\theta_{pq} = 0^\circ$ and passes through the high- p_m tail at large θ_{pq} and p_m . The $x_{Bj} = 0.6$ curve roughly marks out the high- p_m limit of the distribution for a particular value of θ_{pq} . Fig. 4 shows the same attributes for the normal torus polarity data. In this plot we did choose different values of Q^2 and x_{Bj} because those distributions are different for the kinematics here.

2) Only if it is not too much work: As I said, I would prefer a calculation where both the numerator and the denominator of the Born asymmetry as well as of the radiated asymmetry are simulated as a function of ALL variables (Q^2 , p_{miss} , \cos_{th} , ϕ) over a 4-D grid within the envelope of your cuts, and then averaged for each of your bins (weighted by data) to

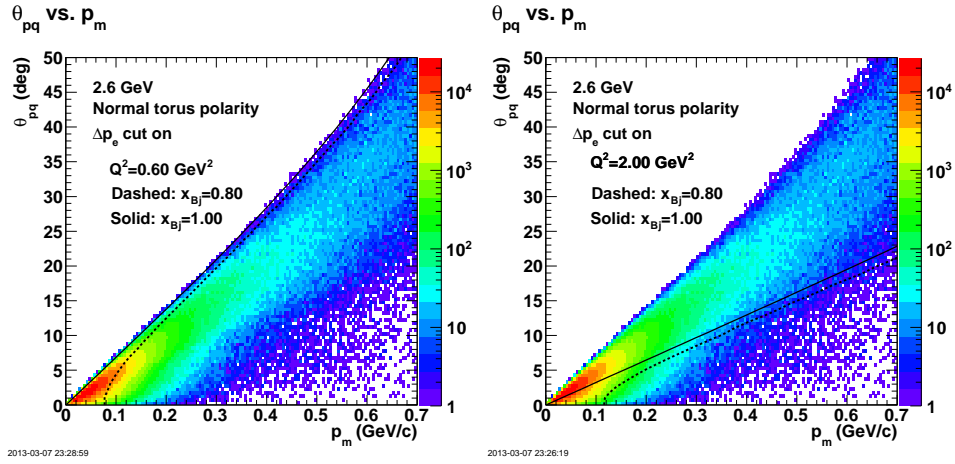


Figure 4: Same as the previous plot except normal torus polarity data and different kinematic curves.

calculate the model Born Asymmetry and the model radiated asymmetry for each of your p_m bins (you obviously already do this for the Born asymmetry, using WvO's model). Then, I would apply just the difference between the two (born - radiated) to your measured asymmetry to get the Born asymmetry. This way, you avoid possible divisions by zero and also the unequal weighting of events which is an unavoidable consequence of event-by-event corrections. As a minimum, it would be very illustrative to see if the answer comes out differently than with your method - such a difference could be a good estimate of this particular systematic uncertainty.

The first step in doing the radiative corrections (RCs) this way is to essentially change variables. The RC code we use called EXCLURAD calculates the correction as a function of W , Q^2 , $\cos \theta_{pq}$, and ϕ_{pq} . I think you want that calculation to be a function of p_m , Q^2 , $\cos \theta_{pq}$, and ϕ_{pq} . To do that we need to calculate W as a function of p_m , Q^2 , $\cos \theta_{pq}$, and ϕ_{pq} . I have included an appendix below that shows the relevant equations taken mostly from Ref. 11 of the analysis note along with a plot of the functions relating p_m to W for different choices of $\cos \theta_{pq}$ and $Q^2 = 0.2 \text{ GeV}^2$.

If I understand what you are asking, you would like to see a GSIM simulation using an event generator based on (1) WVO's model and (2) WVO's model modified by radiation calculated in EXCLURAD. The output of each simulation would be passed through our analysis chain to produce A'_{LT} and the difference between the two would be added to our measured A'_{LT} . It's worth pointing out that the radiative corrections as calculated now are small compared to the statistical uncertainty of our data. Figure 5 shows the difference between A'_{LT} extracted with and without radiative corrections and then divided by the statistical uncertainty on the measured A'_{LT} . The ratio is small across the full range of p_m even at low missing momenta where the measured A'_{LT} and the statistical uncertainty are typically small. If the plan I have outlined above is correct, that will take some time to do, but if you and the committee think it's needed, then we will do it.

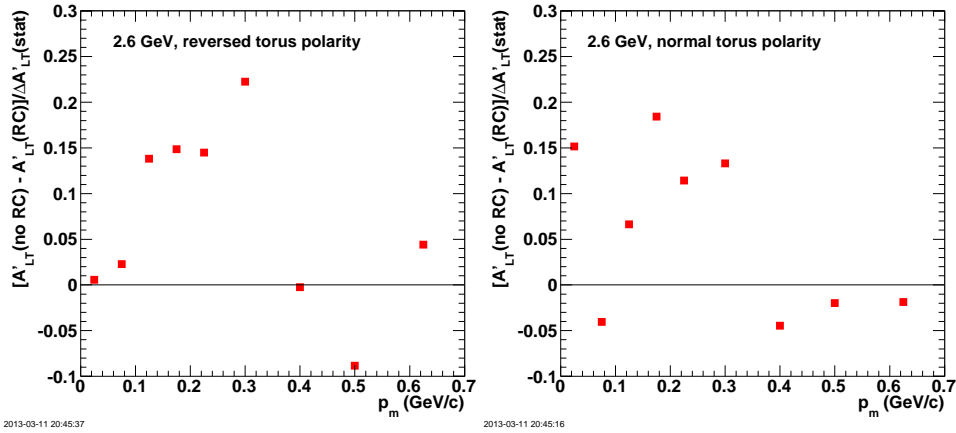


Figure 5: Ratio of the difference between A'_{LT} with and without radiative corrections divided by the statistical uncertainty of the measured A'_{LT} .

Beyond that, I am still unconvinced that you need the cut on $p(e')$ - if radiative corrections are small and well done, why avoid that region? On the other hand, I would think that the measured asymmetry might well depend on $\cos(\theta_{nq})$ quite significantly (which is what we found for A) - ideally, I would have preferred a binning of the data in three $\cos(\theta_{nq})$ bins (backward, e.g. < -0.3 ; sideways, $-0.3 < \cos < 0.3$; forward, > 0.3). But I understand I may be asking for too much here

For the first question: The long tail in Fig 9 of the analysis note (and reproduced below) can come from events with low momentum AND low angle. Collisions where photons are radiated after the collision (so the electron is going at least roughly in the unradiated electron direction) will have lower-than-expected momentum. Events that radiate a photon before the

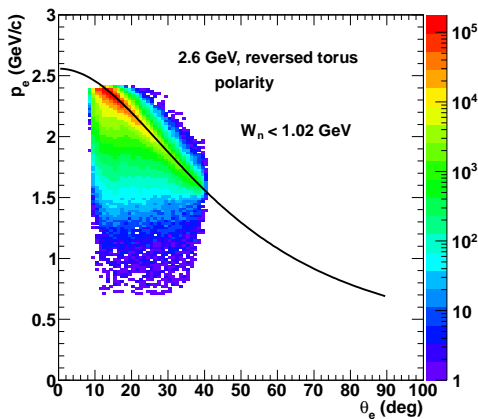


Figure 6: Scattered electron momentum p_e versus scattering angle θ_e for QE events and reversed torus polarity. The black curve is for elastic scattering off the proton.

collision will produce electrons with lower-than-expected momenta AND distorted angles. The EXCLURAD calculation corrects for both cases including the interference between them. If we took off the Δp_e cut and integrated over all p_e we would be mixing in events from the wrong momentum or angle bins due to events where the photon was radiated before the collision with the target. As the photon energies get larger, we have to rely more on the calculations of the radiative corrections which rely, in turn, on our understanding of the nuclear physics at increasingly different kinematics from quasielastic scattering. The Δp_e cut reduces ambiguities in the interpretation of the results at kinematics far from the quasielastic peak and has limited effect on the quality of our statistics. In other words, your suggestion may work for events where the photon was radiated after the collision with the target so the electron angle is closer to the one expected for a scattered electron with no radiated photons. However, things are different when the photon is radiated before the collision with the target because both angle and momentum are now different from their values for unradiated events.

For the second question: I agree that we should see a strong dependence in the asymmetry on θ_{pq} . However, for a quasielastic event with a given Q^2 , x_{Bj} and p_m there is only a small range of θ_{pq} that is allowed. Consider the solid curves in Figures 3 and 4. They show the value of θ_{pq} as a function of p_m for a particular value of Q^2 and two choices of x_{Bj} . Nearly all of the quasielastic events for each Q^2 lie in the region between those two curves. Consider, for example, the right-hand panel of Figure 4. Events with $Q^2 = 0.2 \text{ GeV}^2$ and missing momentum in the range $p_e = 0.3 - 0.4 \text{ GeV}/c$ have to come in the range $\theta_{pq} = 8^\circ - 12^\circ$. Once you have the missing momentum at some Q^2 , there is not much choice in what you have for θ_{pq} . To build a bit more on this point consider Fig. 7. We extracted A'_{LT} with cuts on the value of $\cos \theta_{pq}$. For $\cos \theta_{pq} > 0.3$ as recommended in the comment there was no change in A'_{LT} . We did not see any significant impact until $\cos \theta_{pq}$ was close to one, the effect of a $\cos \theta_{pq} > 0.95$ cut is shown. The missing momentum and $\cos \theta_{pq}$ (and θ_{pq}) are tightly correlated with one another see Figs 3-4). As you remove events with ‘small’ $\cos \theta_{pq}$ (corresponding to large θ_{pq} and p_m) you are removing only large p_m events. The low- p_m A'_{LT} in Fig. 7 is unchanged while the large- p_m A'_{LT} changes significantly and loses events making

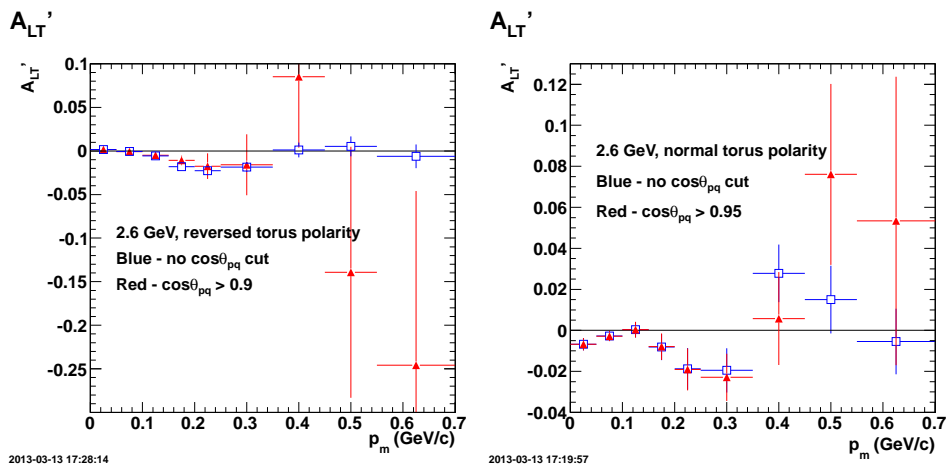


Figure 7: Impact of cuts on $\cos \theta_{pq}$ on A'_{LT} .

the statistical uncertainties much larger.

APPENDIX: Getting W as a function of p_m , Q^2 , $\cos \theta_{pq}$, and ϕ_{pq} .

At the risk of repeating ourselves we start with the equation for p_m (Equation 2.19 in Ref. 11)

$$p_m = \sqrt{\left(\frac{q_L}{2} + p \frac{E_W}{W} \cos \theta_{pq}^{cm}\right)^2 + p^2 \sin^2 \theta_{pq}^{cm}} \quad . \quad (1)$$

The components of p_m are p (proton/neutron 3-momentum in the center of mass)

$$p = \sqrt{\frac{[W^2 - (m_p + m_n)^2][W^2 - (m_p - m_n)^2]}{4W^2}}, \quad (2)$$

where m_p and m_n are the proton and neutron masses respectively and

$$E_W = M_d + \nu = M_d + \frac{W^2 + Q^2 - M_d^2}{2M_d} \quad (3)$$

where M_d is the deuteron mass and

$$q_L = \sqrt{E_W^2 - W^2} \quad . \quad (4)$$

We want the angles in the lab so we start with

$$\tan \theta_{pq}^{lab} = \frac{\sin \theta_{pq}^{cm}}{\gamma \left(\frac{v_{cm}}{v_p^{cm}} + \cos \theta_{pq}^{cm}\right)} \quad (5)$$

and invert this to obtain a quadratic equation in $\sin \theta_{pq}^{cm}$ which yields

$$\sin \theta_{pq}^{cm} = \frac{\frac{2v_{cm}}{\gamma v_p^{cm} \tan \theta_{pq}} \pm \sqrt{\left(\frac{2v_{cm}}{\gamma v_p^{cm} \tan \theta_{pq}}\right)^2 - 4 \left(1 + \frac{1}{\gamma^2 \tan^2 \theta_{pq}}\right) \left(\left(\frac{v_{cm}}{v_p^{cm}}\right)^2 - 1\right)}}{2 \left(1 + \frac{1}{\gamma^2 \tan^2 \theta_{pq}}\right)} \quad (6)$$

where

$$\gamma = \frac{E_W}{W} \quad v_p^{cm} = \frac{p}{\sqrt{p^2 + m_p^2}} \quad v_{cm} = \frac{q_L}{E_W} \quad (7)$$

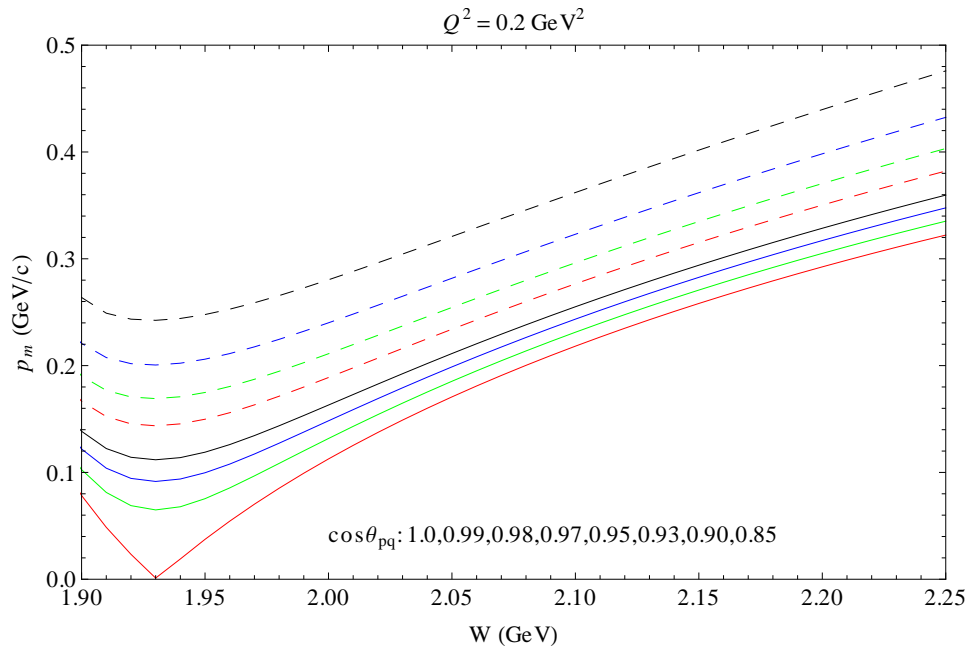


Figure 8: Plot of curves showing relationship between W , $\cos\theta_{pq}$, and p_m for $Q^2 = 0.2 \text{ GeV}^2$.